JOURNAL OF MATERIALS SCIENCE **36** (2001) 2061–2066

Glass formation, optical properties and local atomic arrangement of chalcogenide systems GeTe-Cu and GeTe-In

S. A. FAYEK, S. M. EL SAYED, EL-SAYED
National Center for Radiation Research and Technology, Nasr City, Cairo, Egypt
A. MEHANA, A. M. HAMZA
Military Technical College, Cairo, Egypt

Glass-forming regions of ternary Ge-Te-Cu and Ge-Te-In chalcogenide glasses are examined by differential scanning calorimeter and by X-ray diffraction. Glass transition and crystallization temperatures are about 120 °C To 260 °C, respectively higher than those of binary Ge-Te glass [T. Katsuyama and M. Matsumura, "Infrared Optical Fibres" (Adam Hilger, London, 1989) p. 212]. Only a small range of compositions after quenching the melting alloy is characterized by disordered state, but this range of composition is widened when using a vapor deposition technique. These compositions have two glass transition temperatures, showing the existence of phases in the sample. Both the Kissinger equation and modified Kissinger kinetic analysis were adopted to estimate activation energy and the reaction order of the process. Ge-Te-Cu and Ge-Te-In crystallized in two stages, nucleation and crystal growth. These two processes can be distinguished by exothermal crystallization patterns. An atomic radial distribution analysis has been made on bulk $Ge_1Te_4In_x$ and $Ge_1Te_4Cu_x$ with $x = 0.1$ by X-ray diffraction techniques. The radial distribution function (RDF) is discussed in terms of the structure factor $F(s)$. Thin films of Ge-Te-Cu and Ge-Te-In are deposited on silicate glass and silicon wafer substrates by vacuum evaporation. The optical energy E_{opt} are determined from transmission and reflection data of a deposited films. The value of E_{opt} decreased by increasing metal additive such as Cu or In and discussed as a function of the conditions of their preparation such as substrate type.

1. Introduction

Infrared optical fibers operating at 2–12 μm in wavelength are required for infrared sensing applications such as radiometric thermometry, and CO_2 laser power applications such as laser surgery [1]. The Te- based chalcogenide glasses are used for such applications because their infrared absorption edges are located in a wave length region above 12 μm [2]. However, only a few compositions such as Ge-Te and As-Te based glasses have been investigated as memory switching glasses [3–7]. In this manuscript, ternary Ge-Te-Cu and Ge-Te-In compositions were studied for use as infrared optical fiber material.

The study of glassy material is currently being strongly driven by the application of calorimetric techniques; through differential scanning calorimeter (DSC), it is possible to penetrate the glass-forming mechanisms, determining kinetic parameters which describe the phenomena of nucleation and subsequent crystalline growth, from amorphous materials. The knowledge of the factors which influence the glass-crystal reactions leads to a better control of the inverse reactions and, therefore, of the properties and synthesis of amorphous materials. Studies of kinetics are always connected with the concept of activation energy. The value of this energy in glasses is associated with nucleation and growth mechanisms that dominate the devitrifications of most glassy solids. Studies of the crystallization of glasses upon heating can be performed in several different ways, isothermal and non-isothermal.

The atomic structure of these solids is not completely random, as happens with gases, as the cohesion due to their chemical bonds must be present among their atom [8]. The atoms must be in contact with each other, and there is short-range order. The structural units formed by an atom and its nearest neighbors corresponds, in away, to the unit cell of a crystal. The atomic distances and bond angles in each of these structural units are not, determined, but take a certain distribution of values and unlike in a crystalline network, the repetition of structural units is not periodic, and the orientation and structural characteristics of the clusters is different in each direction. An amorphous solid, therefore, exhibits more variety than a crystal, infinitely increasing the technological possibilities of glasses. The energy of an amorphous material is located in a relative minimum, which is why the posses are based on saving the energetic excess they posses in relation to the same crystalline alloy

[9]. Although it was thought that the property of turning into glass was restricted to substances with a very wide band gap, we can now state that this property is common to condensable material in general, if subjected to suitable treatment [10]. Analysis of the optical absorption spectra is one of the most productive tools for understanding and developing the energy band diagram of both crystalline and amorphous materials.

An important step will be taken when a definite relationship is found between the structural characteristics and thermal behavior of glasses; some hypotheses have already been formulated in this sense [11, 12] and verified on chalcogenide materials.

2. Experimental detail

Bulk amorphous $Ge_1Te_4In_x$ and $Ge_1Te_4Cu_x$ with ($x = 0.05$ and 0.1 at.%) were prepared from highly pure Ge, Te, Cu and In (99.999%) purity loaded into a fused silica tubes, which were evacuated (10^{-5} torr) and sealed off then heated at 850°C for 8 hrs and shaken several times to ensure complete homogeneity. The molten materials were quenched in saturated aqueous solution of NaCl at around –15 °C. The scanning electron microscope (Joel SE M-5400) with a link exl EDX detector (electron dispersion x-ray) was used to determine the chemical compostion of samples, fully quantitative analysis results were obtained from the spectra by processing the data through Zaf correction program.

The alloys were ground to a fine powder for the differential scanning calorimetry studies and samples weighing 25 mg were placed in closed aluminum pans and heated at 500°C in a Shimadzue model (DT-50) differential scanning calorimetry (DSC). Heating rates of 5, 10, 15, 20 and 30°C/min were chosen for the study of the crystallization using the multiscanning technique. Standard wide-angle x-ray scattering experiments were performed on X-ray diffraction equipped with a graphite monochromatic scintillation counter and standard associated electronic equipment.

Two sets of four series of intensities collected with Bragg-Brentano geometry in the angle interval $4^\circ \leq 2\theta \leq 140^\circ$ for Cu K_α ($\lambda = 15.4056$ nm) radiation with step size of $(\Delta 2\theta) = 0.2^\circ$, were used from 4° to 70°, and $(\Delta 2\theta) = 0.5^\circ$ from 70° to 140°. Counts were measured by keeping a fixed time interval for purposes of automatic data registration by means of Shimadzue systems. The intensity assigned to each observation point was the mean value of those series measured at that point. Detailed analysis of the atomic arrangement in ternary alloys requires the determination of the radial distribution function. Samples in the form of thin films were prepared by evaporating the synthesized material at a base pressure of 2×10^{-5} torr onto cleaned silicate glass and N-type silicon wafer were used as a substrate using Edward coating unit model 306. A source substrate distance of 12 cm was adjusted during deposition. No internal control of the substrate temperature was preformed. The deposition parameters were kept constant so that a comparison of result could be made under identical conditions. The film thickness (d) was controlled at 200 nm with a quartz crystal monitor and confirmed by the interferometric method [13].

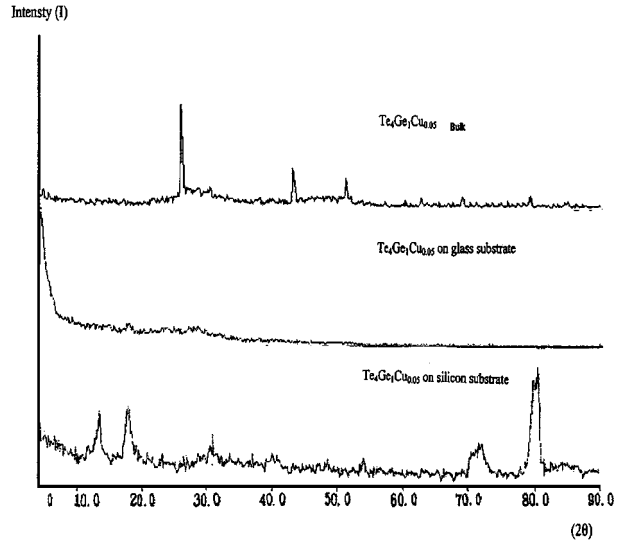

Figure 1 X-ray diffraction patterns of $Ge_1Te_4Cu_{0.05}$ as bulk and thin film.

X-ray diffraction has been used to investigate and characterize the structure of the prepared bulk and films using machine model XD-D series Shimadzu with Cu anode. The transmitance and reflectance of the films were measured using double beam Shimadzu UV-VIS spectrophotometer in the spectral range 200–1100 nm. wavelength.

3. Results

3.1. X-Ray diffraction patterns of $Ge_1Te_4Cu_x$ and $Ge_1Te_4In_x$

The patterns revealed that bulk samples were partially crystalline except $x = 0.05$. Diffuse haloes characterizing the amorphous nature of the films deposited on silicate glass and some diffraction pattern for film deposited on Si wafer are in Fig. 1 as an example.

3.2. Effect of composition and heating rate on thermal transition

Differential scanning calorimeter (DSC) traces at rate of 10 °C/min. of freshly prepared $Ge_1Te_4(Cu_x, In_x)$ where $x = 0.05$ and 0.1 are shown in Fig. 2. The traces follow the known common behavior, where the three characteristic temperatures, glass transition temp. (T_g), crystallization temperature (T_c) and melting temperature (T_m) are observed and given in Table I. For Ge-Te doped by metal such as (Cu, In), two glass transition temp. (T_{g1}, T_{g2}) and one crystallization temperatures (T_{C1}) are almostly observed in the sequence $T_{g1} < T_{c1} < T_{g2}$ [14]. The effect of heating rate on the characteristic temperatures was investigated at five different rates for $In_{0.05}$ and $Cu_{0.05}$ and the data are listed in Table I. The observed T_g decreased by increasing the heating rate, by inspection of obtained data. For an ideal glass there is a lower limit to this change but for this system the wide range of change in Tg indicate that this system behaves as a normal glass. It is worthy mention that for $x = 0.05, 0.1$ at %, the DSC scan for $q = 2c$/min shows that a small amount of the sample material has been crystallized. The crystallization of amorphous material proceeds by the processes

TABLE I Coordination number R, glass-forming tendency K_{g1} and characteristic transition temperature at different rates of the different compositions

Compositions	R	K_{g1}	T_g °C Rate °C/min	T_g T_{g1}	T_g T_{g2}	T_c°C Min	T_c°C T_p	T_m°C Min	T_m°C Mid
			2			187.8	200.0	344.4	350.7
			10	95	280	194.0	216.0	346.0	352.8
$Ge_1Te_4Cu_{0.05}$	2.43	1.22	15			205.2	220.0	341.4	354.2
			20			199.3	222.9	338.0	356.0
			30			193.0	228.6	319.9	359.0
			2			193.1	202.4	343.0	350.5
			5			190.5	209.0	345.7	352.0
			10	141	-	177.0	214.2	337.1	354.0
$Ge_1Te_4Cu_{0.1}$	2.48	1.15	15			191.0	217.0	337.0	354.8
			20			183.6	219.0	339,3	355.5
			30			192.4	222.9	329.0	358.5
			2			189.3	208.5	360.0	370.0
			5			183.3	217.4	363.6	370.6
$Ge_1Te_4In_{0.05}$	2.42	1.90	10	146	257	196.9	220.9	363.5	371.7
			20			218.0	230.0	362.9	363.6
			30			189.0	236.0	352.0	376.1
			2			-	-	-	371.7
			5			-	-	-	389.8
$Ge_1Te_4In_{0.1}$	2.427	-	10	86	243	-	-	-	385.5
			20			-	-	-	392.5
			30			-	-	-	392.7

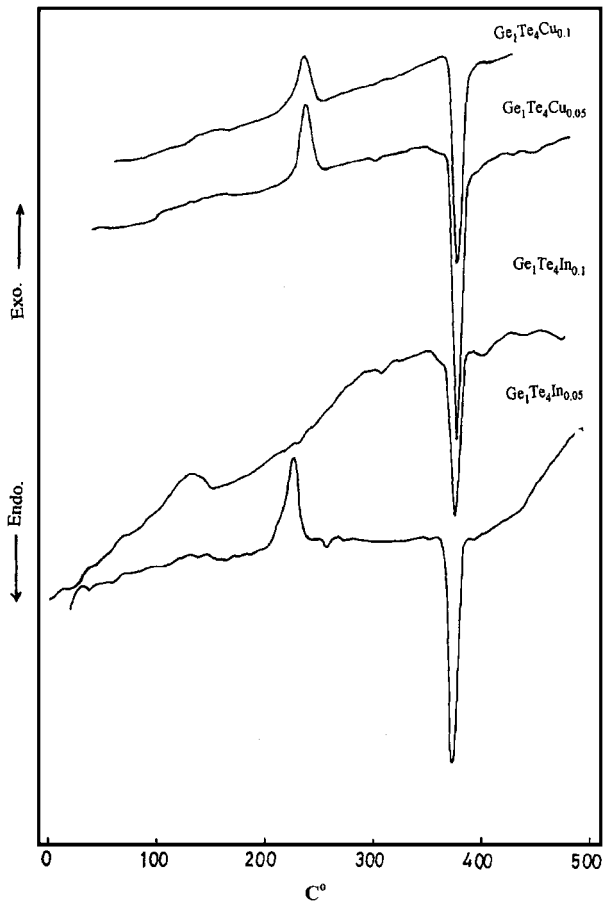

Figure 2 DTA thermograms for at rate 10°C/min for all compositions.

of nucleation and growth. Since growth follows nucleation, in some cases if the nucleation is prevented, there will be no crystallization. However, even if nucleation occurs, the crystallization orates of growth. Turbuull (10) indicates that the growth rate in liquids with high viscosity is limited.

3.3. Crystallization kinetics

The evaluation of non-isothermal activation energy for crystal growth has been estimated by a large number of mathematical treatments based on the formal theories of transformation kinetics. Used theories differ greatly in their assumption and in some cases, they lead to contradictory results, partial area analysis and peak shift analyses are the basic method for all mathematical treatments. However, Marotta *et al.* [19] have recently pointed out the limitation of the single scan technique and showed that it is difficult to calculate the value of E and n by this method. They have suggested that multiple scanning can be used successfully for calculating E and n from the same set of measurements using the theory shape index.

The Kissinger formula has been here used for homogenous crystallization [16] or in other words surface nucleation is dominates that $n = 1$.

$$\mathrm{Ln}\left(\varphi / T_p^2\right) = \{(-E/RT_p) + \mathrm{cons.}\} \qquad (1)$$

The plot of $\mathrm{Ln}(\varphi/T_p^2)$ vs. $(1/T_p)$ which are shown in Fig. 3 are well fitted by straight lines. From the slopes of these lines, the activation of crystallization E can be estimated, and then listed in Table II.

TABLE II The thermal parameters of the ternary glassy $Ge_1Te_4Cu_x$ and $Ge_1Te_4In_x$ where $x = 0.05$ and $x = 0.1$ systems for the crystallization peak, E values are given in eV/atom

Compositions	Kissinger method E, when $n = 1$	Mahadevan approx. E, when $n = m = 1$	Modified Kissinger method E	n	m
$Ge_1Te_4Cu_{0.05}$	3.857	4.084	3.857	1	1
$Ge_1Te_4Cu_{0.1}$	4.991	5.128	5.748	2	1
$Ge_1Te_4In_{0.05}$	4.511	4.899	6.464	2	1

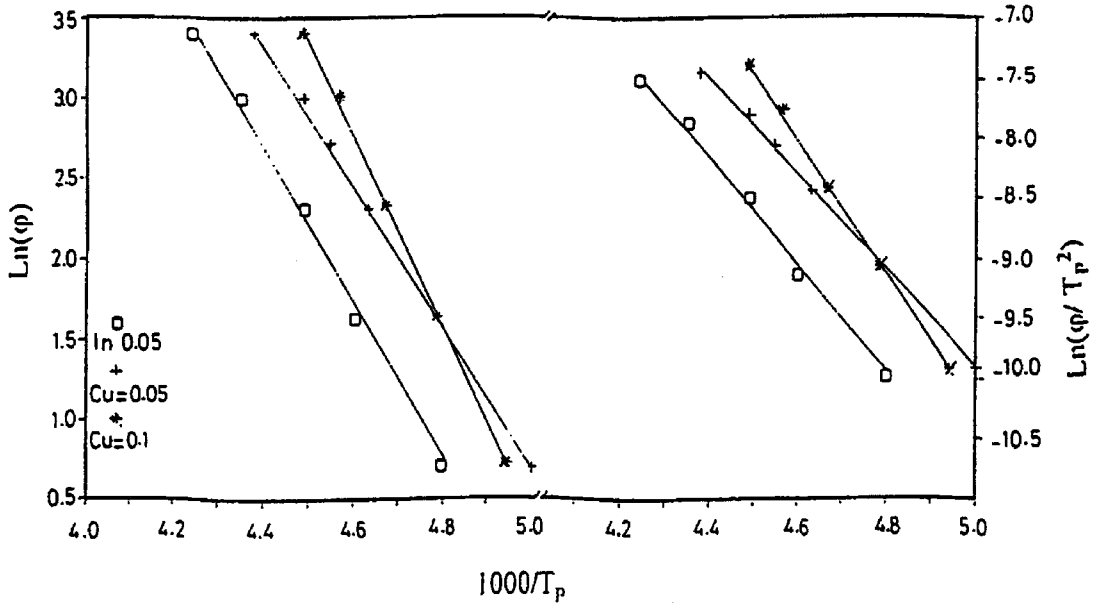

Figure 3 The relation between $[\ln(\varphi/T_p^2)]$ aginst $10^3/T_p$ (Kissinger method) and $[\ln(\varphi)]$ against $10^3/T_p$ (Mahadevan appro. Method) for different compositions.

The Mahadeven *et al*. approximation [15] was used, where the variation in $\mathrm{Ln}(1/T_p^2)$ with $\mathrm{Ln}\,\varphi$ is much less than that in $(1/T_p)$ with $\mathrm{Ln}\,\varphi$. Therefore Equation 1 can be written in the form

$$\mathrm{Ln}(\varphi) = (-E/RT_p) + \text{const.} \tag{2}$$

A plot of $\mathrm{Ln}(\varphi)$ vs. $(1/T_p)$ for $Ge_1Te_4(Cu_x, In_x)$ with $x = 0.05$ and 0.1 at % gave a straight line, as shown in Fig. 3. The values of E obtained from the above method are listed in Table II.

The modified Kissinger-method: In this method the relation between the rate φ and crystallization temperature T_p is assumed to have the following form.

$$\mathrm{Ln}\left(\varphi^n/T_p^2\right) = (-mE/RT_p) + \text{const.} \tag{3}$$

If the crystallization mechanism is known precisely and does not change with the heating rate, the plot of $\ln(\varphi^n/T_p^2)$ vs. $(1/T_p)$ for $x = 0.1$ gives the value of mE. Dividing mE by m, the activation energy for crystal growth can be obtained and listed in Table II. Only when the surface nucleation is dominant, in other words, $n = m = 1$ for all heating rate the Equation 3 is identical with so-called Kissinger Equation [20].

$$n = 1.26(a/b)^{1/2} \tag{4}$$

Therefore, from Table II, the corresponding values of m are equal to 1.

3.4. Effect of composition and substrate on the optical energy gap

In order to determine the absorption coefficient (α) by measuring the reflectance R and the transmittance T and knowing the film thickness d, the following equation has to used [21].

$$\alpha = (1/d)\ln[(1-R)^2/T] \tag{5}$$

The absorption coefficient $\alpha(\omega)$ was calculated as a function of wavelength using (5). The absorption coefficient $\alpha(\omega)$ less than 10^{-4} cm^{-1} many amorphous semiconductors show an exponential dependence on photon energy $h\omega$ and obey by Tauc *et al.* [22], and discussed in more general terms by Davis and Mott [23] whose equation was of the form

$$\alpha(\omega) = \beta(h\omega - E_{\mathrm{opt}})^{\gamma}/h\omega \tag{6}$$

where β^{-1} is band edge parameter, γ is number that characterize the transition process and E_{opt} is the optical gap.

In non-crystalline systems the non-direct transitions are most likely to occur due to the absence of translation symmetry and $\gamma = 2$ or 3 for allowed or forbidden non-direct transition. The present result were found to obey [24] with $\gamma = 2$. Optical energy gap has been estimated from linear plots of $(\alpha h\omega)^{1/2}$ against $h\omega$ as shown in Fig. 4. The obtained data shows that the variation of E_{opt} and E_e with Cu or In additive and kind of substrate as shown in Table III.

3.5. Radial distribution function (RDF)

The observed intensities were corrected for background, polarization, and multiple scattering and were normalized into units (e.u) by the high-angle method [25] and, subsequently, the incoherent scattering was subtracted.

TABLE III The optical properties of thin film glasses compositions and peak position of the RDF for bulk compositions

Compositions	E_{opt} Glass	E_{opt} Silicon	Frist peak (A^0)	Area (atoms)	Frist peak (A^0)	Area (atoms)
$Ge_1Te_4Cu_{0.05}$	1.055	2.832	----	----	-----	-----
$Ge_1Te_4Cu_{0.1}$	0.722	2.500	2.880	2.113	4.280	5.893
$Ge_1Te_4In_{0.05}$	1.351	2.000	-------	-----	-----	------
$Ge_1Te_4In_{0.1}$	1.000	1.500	2.880	2.113	4.640	5.185

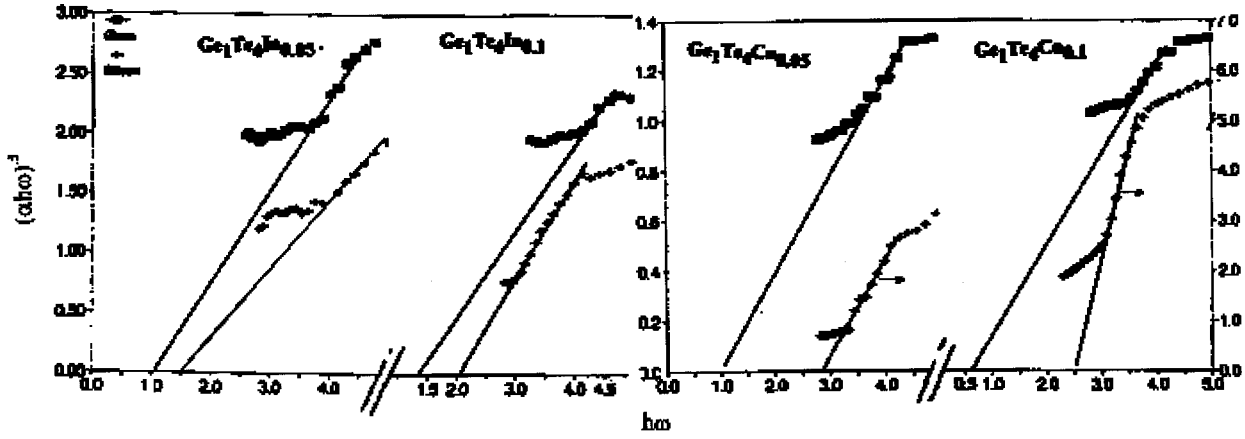

Figure 4 Dependence of $(\alpha h\omega)^{1/2}$ on the photon energy $h\omega$ (eV) for $Ge_1Te_4(\text{ln or Cu})_x$ films where $x = 0.05$ and $x = 0.1$.

The RDF is calculated as follows:

$$4\Pi r^2\rho(r) = 4\Pi r^2\rho_0(r) + rG(r) \tag{7}$$

where $\rho_0(r)$ and $\rho(r)$ represented the mean atomic distribution and the local atomic density, respectively, and $G(r)$ stands for the Fourier transformation of a function of experimental intensities, being

$$G(r) = \int_0^{\text{SMAX}} F(s)\sin(sr)\,ds \tag{8}$$

with *s* being equal to the scattering vector modulus, and *F(s)* being the interference function given by

$$F(s) = \text{Si}(s) \tag{9}$$

with *i(s)* being a function given by

$$I(s) = \left[I_{\text{e.u}-}\Sigma\chi_i f_i^2\right]/[\Sigma\chi_i f_i]^2 \tag{10}$$

where χ_i is the atomic fraction of the I element and f_i the atomic scattering factor with $i =$ Cu,Ge,Te or In, Ge,Te and $I_{\text{e.u}}$ represent the resulting intensity values in electronic units after correction. The RDF after the above- mentioned procedure have been plotted for both samples as shown in Fig. 5.

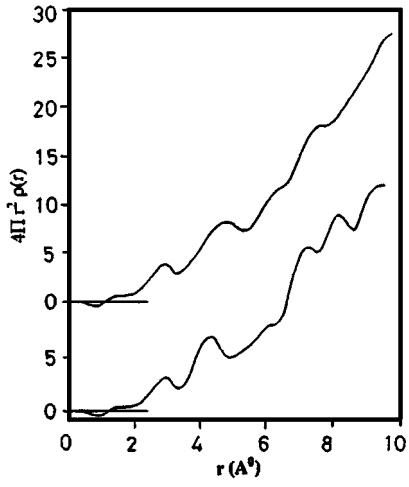

Figure 5 Reduced RDF from scattering experiments for bulk glassy compositions $Ge_1Te_4Cu_{0.1}$ and $Ge_1Te_4\,ln_{0.1}$.

4. Discussion

1. The obtained results of X-ray diffraction patterns of the investigated bulk samples and thin film are show in Fig. 1. This figure reveals that for bulk samples are shown in partially crystalline except for $\text{In} = 0.05$ but for thin film deposited on silicate glass has no diffraction peak. In addition the diffraction peaks for films deposited on silicon wafer represented a layer of SiO_2 determination by comparing ASTM card of SiO_2.

2. Increasing the heating rate decreases the observed T_g. That we can say the wide ranges of changes in T_g indicate that this system behaves as a normal glass and not ideal glass, which characterized by low limit of this change.

3. For $Ge_1Te_4In_x$ or $Ge_1Te_4Cu_x$ $0.05 \leq x \leq 0.1$ glass transition temperature T_{g1}, T_{g2} were generally observed in the sequence $T_{g1} < T_{C1} < T_{g2}$ [14]. This is explained by the rejection of germanium atoms into the surrounding glass during the primary crystallization; the composition of the alloy therefore changes during heating, and the glass transition temperature shifts from T_{g1} to T_{g2} except for high heating rate such as 20 °C/min, 30 °C/min. T_{g2} canceled indicate more homogeneity than low speed.

4. By increasing the heating rate the crystallization temperature increased due the reduction in a crystal growth and it is worthy mention that $\varphi = 2$ C/min a small crystallization peak T_c indicating that small amount of the sample material has been crystallized. That we can say the crystallization of amorphous material controlled by the nucleation followed growth as a result, the crystallization rate is suppressed by reducing the rate of nucleation or the rate of growth. Since growth follows nucleation, in some cases if the nucleation is prevented, there will be no crystallization. However, even if nucleation occurs, the crystallization rate can still be suppressed by reducing the rate of growth. Turnbull[10] indicates that the growth rate in liquids with high viscosity is limited.

5. It can be seen that In additive in the Ge-Te glasses decreases T_g than the Cu additive. Therefore, it is clear that Ge-Te-Cu glasses are more stable than Ge-Te-In glasses.

6. Multiscan techniques, were applied to evaluate the activation energy (E), the order (n) of Crystallization and the order of crystal growth. The activation energy

of crystallization is increased by increasing the metal additive (In or Cu) and this means that the bond strength and coordination number increased by metal additive. The crystallization mechanisms of glass are surface and one-dimensional crystallization process.

7. We can noticed that the transmission for films evaporated upon glass substrate represented a negligibly amount comparing with films on Si substrate consequently the films deposited Si wafer having higher absorption coefficient than films on glass substrate. This trend may be due to variety in grain size and layer of SiO_2[26].

8. Obtained results allow concluding that the conduction in the chalcogenide glasses $Ge_1Te_4In_x$ and $Ge_1Te_4Cu_x$ with $0.05 \leq x \leq 0.1$ due to allowed indirect transition. E_{opt} for In addive more effective than Cu additive that in both silicate glass and Si wafer substrate. This result is due to a large atomic radius and high electronegativity According to the result we except that evaporation upon Si wafer reduced the defect states than in glass substrate.

9. RDF in Fig. 5 show small peaks at $r = 0.06$ nm. The peak is spurious as no legitimate peak can occur at an r smaller than the sum of the smallest pair of atomic radii involved.

The area under the first peak in the RDF is a measure of the number of nearest neighbours about an atom. In the present work the area has been calculated by considering the right hand side of the first peak to the symmetrical to the left-hand side. This method minimises the contribution from atoms in other coordination shells [27]. The results are given in Table IV. RDF of $Ge_1Te_4In_{0.1}$ and $Ge_1Te_4Cu_{0.1}$ for powder exhibit a prominent peak and a few other sharp peaks. The sharpness of the peak may be attributed to the fact that a creation extent to crystalline states and there by a long -range periodic rearrangement of atoms is achieved. The positions (r_1) of the maxim of the peaks in RDFs are give in Table III. The position and area of the first proper peaks of RDF corresponded to the Ge-Te [29, 30] that is to say that Strong correlation between Ge-Te atoms, The interatomic distance from the first peak were 2.88 nm for Ge-Te. Structure representation has demonstrated that there are Te-Cu, Te-In and Te-Te bonds but not Ge-Ge bonds, which result from the smaller binding energy of Ge-Ge [31] compared with Ge-Te, Te-Cu, Te-In and Te-Te.

5. Conclusion

The glass transition temperature of ternary Ge Te Cu glasses is greater than Ge Te In which makes the first system more available in several application

It was concluded that the crystallization mechanism should be taken into account for obtaining the meaningful activation energy.

According to the above we can be sure that films on the two different substrates characterized by short-range order but the grain size differs.

It is seen that the position of the fundamental absorption edge shift to the higher wavelength by adding Cu or In indicating the possibility of these glasses beings used as infrared optical fiber material applications.

References

1. T. KATSUYAMA and H. MATSUMURA, "Infrared Optical Fibers" (Adam Hilger, London, 1989) p. 212.
2. *Idem., Appl. Phys. Lett.* **49** (1986) 22.
3. T. TAKAMORI, R. ROY and G. J. MCCARTHY, *Mater. Res. Bull.* **5** (1970) 529.
4. S. LIZIMA, M. SUGI, M. KIKUCHI and K. TANAKA, *Solid State Commun.* **8** (1970) 153.
5. J. A. SAVAGA, *J. Mater. Sci.* **6** (1971) 964.
6. *Idem. J. Non-Crystalline Solids* **11** (1972) 121.
7. S. BORDAS, J. CASAS-VAZQUEZ, N. CLAVAGUERA and M. T. CLAVAGUERA-MORA, *Thermochim. Acta* **28** (1973) 387.
8. R. A. LIGERO, M. CASAS-RUIZ, J. VAZQUEZ and P. VILLARES, *J. of Mater. Sci.* **27** (1992) 1001.
9. A. E. OWEN, in "Electronic and Structural Properties of Amorphous Semi.-Conductor" edited by P. G. Lecomber and J. Mort (Academic, London 1973).
10. J. TAUK, in "Amorphous and Liquid Semi.-Conductor" edited by J. Touc (Plenum Press, New York, 1974) chap. 4.
11. R. A. LIGERO, Ph.D. thesis, University of Cadiz, Spain, 1988.
12. J. S. BERKES, in Non-Crystalline Solids, 4th International Conference, 1977, p. 405.
13. S. TOLANSKY, "*Multiple Beam Interferometry of Surfaces and Films*" (Oxford University Press London) 1947, p. 147.
14. S. ASOKAN, G. PARTHASARATHY and E. S. R. GOPOL, *J. Non-Crystalline Solids* **86** (1986) 48.
15. S. MOHADEVAN, A. GIRIDHAR and A. K. SINGH, *ibid.* **88** (1986) 11.
16. KISSINGER, *Anal. Chem.* **29** (1957) 1702.
17. N. RYSAVA, T. SPASOV and L. TICHY, *J. Therm-Anal.* **32** (1987) 1015.
18. H. YINNON and D. R. UHLMANN, *J. Non-Crystalline Solids* **54** (1983) 253.
19. A. MAROTTA, S. SAIELLO and BURI, *ibid.* **57** (1983) 473.
20. E. KISSINGER, *J. of Research of National Bureau of Standards* **57** (4) (1956) 217.
21. F. DEMICHELLIS, G. KANIAAKIS, A. TAGLIAFERRD and E. TRESSO, *Appl. Optics* **26** (1987) 1737.
22. J. TAUC, R. GRIGOROVICI and A. VANCU. *Phys. Stat. Sol.* **15** (1966) 627.
23. E. A. DAVIS and N. F. MOTT, *Phil. Mag.* **22** (1970) 903.
24. S. R. OVSHINSKY, in "Physical Properties of Amorphous Materials" edited by D. Adler, B. B. Schwartz and M. C. Steel, Institute for Amorphous Studies Series Vol. 1 (Plenum, New York, 1985), Chapt. 2.
25. B. E. WARREN, "X-Ray Diffraction" (Addision-Wesley, Reading MA, 1969).
26. NORIKAZU OHSHIMA, *J. Appl. Phys.* **79** (1996) 11.
27. K. FURUKAWA, B. R. ORTON, J. HAMOR and G. I. WILLIAKS, *Phil. Mag.* **8** (1963) 141.
28. D. HERNDERSON and F. HERMAN. *J. Non-Crystalline Solids* **8/10** (1972) 359.
29. A. CHEVY, A. KUHN and M. S. MARTIN, *J. Cryst. Growth* **38** (1977) 118.
30. S. R. OVCHINSKY and D. ADLER, *Contemp. Phys.* **19** (1978) 109.
31. J. BICERANO and S. R. OVSHINSKY *J. Non-Crystalline Solids* **74** (1972) 75.

Received 16 September 1999
and accepted 24 August 2000